PHYSICAL REVIEW B VOLUME 33, NUMBER 4 15 FEBRUARY 1986

Frequency shifts of vibrational and rotational states of dilute H_2, D_2, and HD impurities in solid Ar under pressure

B. Silvi
Laboratoire des Spectrochemie Moleculaire, Université Pierre et Marie Curie, F-75230 Paris Cédex 05, France

V. Chandrasekharan and M. Chergui
Laboratoire des Interactions Moléculaires et Haute Pressions du Centre National de la Recherche Scientifique, Université de Paris—Nord, F-93430, Villetaneuse, France

R. D. Etters
Department of Physics, Colorado State University, Fort Collins, Colorado 80523

(Received 13 June 1985)

The frequency shifts of the vibrational and rotational transitions of H_2, D_2, and HD molecules trapped in solid Ar are calculated at zero temperature and at pressures $0 \le P \le 373$ kbar. It is found that the pure vibrational and rotational-vibrational transition frequencies are strongly red-shifted in the solid at $P=0$, compared to gas-phase values, and the agreement with Raman scattering measurements is generally good. The calculated pure rotational transitions also show a small red shift at $P=0$ in the solid and are in generally good agreement with the measurements of Jodl and Bier, but less so with those of Prochaska and Andrews, who, except for D_2(Ar), measure small blue shifts. The calculated local-mode frequencies of the impurity molecules in the solid at $P=0$ are also in good agreement with experiment, especially when thermal corrections are considered. With increasing pressure all transition frequencies and the local-mode frequencies are strongly blue-shifted with respect to $P=0$ solid values.

I. INTRODUCTION

The vibrational and rotational spectra of H_2, D_2, and HD impurities in solid argon have previously been measured at various temperatures under zero external pressure using Raman[1,2] and infrared absorption techniques,[3-6] and ir measurements of H_2 in argon have been extended to $P=11$-kbar pressure.[7] Most of the transition frequencies measured by the two Raman experiments[1,2] differ by an amount apparently outside of experimental uncertainty. There is also a divergence of values reported from the ir works.[3-6] All agree, however, that the pure vibrational and vibrational-rotational transition frequencies show strong red shifts in the solid at $P=0$, compared to their gas-phase values. Also measured[2] were the local-mode frequencies of H_2 and D_2 in solid Ar.

In a previous calculation, Vitko and Coll[8] determined the pure vibrational $Q_1(0)$ frequency shifts and the local-mode frequencies of $X=H_2$, D_2, and HD in solid Ar at $P=0$. Their calculated $Q_1(0)$ frequencies were red-shifted considerably more than is indicated by experiment, but the agreement is reasonably good considering that the X-Ar potential they used was a more primitive version of the one used in this work. In their calculation they ignored the distortion of the lattice around the impurity and the anisotropic part of X-Ar potential. Both approximations we will show are reasonable at $P=0$ in the solid. Their calculated local-mode frequencies are in good agreement with experiment.[2]

In this work a different technique is used to extend the calculation to include the pure vibrational, pure rotational, and rotational-vibrational transition frequencies of H_2, D_2, and HD impurities substitutionally trapped in solid Ar at pressures $0 \le P \le 373$ kbar. The local-mode frequencies of the impurities have also been calculated at all pressures. Central to this calculation is the use of an improved version of the X-Ar potential, derived by LeRoy and Carley,[9] a relaxation to equilibrium of the first 16 shells of Ar atoms around the molecular impurity, and the use of terms up to seventh order in a power-series expansion of the hydrogen intramolecular potential[10] in terms of the displacement of the bond length about equilibrium. The zero-point oscillations of the impurity molecule and the host lattice atoms are calculated using a Hartree approximation. At $P=0$, where contact with experiment exists, the calculated results are in substantially better agreement with observed data[1,2] than was the case with previous calculations,[8] and transition frequencies heretofore not calculated also agree well with experiment. At high pressures, strong blue shifts of all the modes are reported.

II. FORMULATION

For a single molecule $X=H_2$, HD, or D_2 isolated in an argon matrix, the Hamiltonian can be expressed as

$$H=H_{\mathrm{Ar}}+H_X+V_{\mathrm{Ar}\text{-}X}\ , \tag{1}$$

where

$$H_{\mathrm{Ar}}=-\frac{\hbar^2}{2M}\sum_{i=2}^{N}\nabla_i^2+\frac{1}{2}\sum_{i=2}^{N}\sum_{j=2}^{N}V_{\mathrm{Ar}}(R_{ij})\ , \tag{2}$$

$$H_X = -\frac{\hbar^2}{2m}\nabla_1^2(R_1) - \frac{\hbar^2}{2\mu}\nabla_\xi^2 + B(\xi)\hat{J}^2 + V_{\text{intra}}(\xi) \,, \tag{3}$$

$$V_{\text{Ar-}X} = \sum_{j=2}^{N} V(R'_{1j}, \theta_{1j}, \xi) \,, \tag{4}$$

where m, M, and μ are the X, Ar, and reduced-X masses, respectively. The rotational kinetic energy operator of the X molecule is $\hat{J}^2$, $\xi = (r - r_e)/r_e$, where r is the instantaneous bond length of the X molecule in the solid lattice and r_e is its gas-phase value.[11] The index $i = 1$ always refers to the X molecule and $i = 2, 3, \ldots, N$ refers to the host lattice argon atoms. The $\mathbf{R}_1$ specifies the position of the X-molecule mass center, R_{ij} is the distance between mass centers of particles (i,j) and θ_{1j} is the angle between the molecular axis of molecule X and the vector $\mathbf{R}'_{1j}$, specifying the distance between the charge center of molecule X and the jth host lattice atom. Except for HD, $\mathbf{R}'_{1j} = \mathbf{R}_{1j}$, the distance between mass centers. For HD the mass center is displaced by a distance $r/6$ from the center of the molecular charge distribution. Thus $\mathbf{R}'_{1j} = \mathbf{R}_{1j} + (r/6)\hat{\mathbf{u}}$, where $\hat{\mathbf{u}}$ is the unit vector identifying the location of the mass center with respect to the center of the charge distribution. The rotational constant is given by

$$B(r) = \hbar^2/(2\mu r^2) = \hbar^2/[2\mu r_e^2(1+\xi)^2] \,. \tag{5}$$

Thus, in Eq. (2) the first term gives the kinetic energy of host lattice argon atoms and the second term gives the potential energy between argon atoms. In Eq. (3) the first three terms are the kinetic energies of the X-molecule center of mass (c.m.), intramolecular vibrations, and rotations, respectively. $V_{\text{intra}}(\xi)$ is the intramolecular potential energy. From the work of LeRoy and Carley,[9]

$$V(R'_{1j}, \theta_{1j}, \xi) = \sum_{k=0}^{3} \sum_{\lambda=0,2} V_{\lambda k}(R'_{1j}) P_\lambda(\cos\theta_{1j})\xi^k \,. \tag{6}$$

In Eq. (6) the P_λ are Legendre polynomials. These potentials have been very accurately fit to spectroscopic data, and the range of validity of the ξ dependence has been extended by requiring that the potential agrees with that of He-X in the limit $\xi \to 0$.

The intramolecular potential is

$$V_{\text{intra}}(\xi) = \sum_{i=2}^{7} a_i \xi^i \,, \tag{7}$$

where the parameters a_i are taken from van Kranendonk.[10] The effective Ar-Ar pair potential V_{Ar} is a piecewise fit of calculated results by LeSar,[12] deduced from electron gas calculations. The well and long-range part of the potential is formulated to closely agree with the excellent results of Aziz and Chen, and Barker and Bobetic.[13] It is given by

$$\begin{aligned}
V_{\text{Ar}}(R) &= \epsilon[U_0(r) + U_1(r)] \,, \\
U_0(r) &= \sum_{n=0}^{5} A_n (r-1)^n \exp[\beta(1-r)] \\
&\quad - \sum_{n=0}^{2} \left[\frac{C_{6+2n}}{r^{6+2n}} + \frac{C_9}{r^9} \right] F(r) \,, \\
U_1(r) &= \begin{cases} [A_6(r-1)^4 + A_7(r-1)^5]\exp[\beta(1-r)], & r > 1 \\ 0, & r \le 1 \end{cases} \\
F(r) &= \begin{cases} \exp[-(d/r-1)^{3/2}], & r < d \\ 1, & r > d \end{cases}
\end{aligned} \tag{8}$$

where $r = R/r_0$, $A_0 = -0.023\,456\,55$, $A_1 = -5.087\,821\,4$, $A_2 = -1.017\,947$, $A_3 = 1.517\,094\,7$, $A_4 = -11.604\,06$, $A_5 = -10.424\,389$, $A_6 = -0.979\,607\,24$, $A_7 = 9.186\,667\,5$, $\beta = 11.25$, $C_6 = 1.067\,262\,3$, $C_8 = 0.582\,610\,9$, $C_9 = -0.091\,032\,8$, $C_{10} = 0.356\,466\,1$, $r_0 = 3.773$ Å, $d = 1.8$, and $\epsilon = 143.224$ K.

An important element in simplifying the calculation is to recognize that the rotational, translational, and intramolecular vibrational degrees of freedom are only weakly coupled to one another. For example, Eq. (6) shows that the angular dependence in the Ar-X potential appears as $P_2(\cos\theta)$. However, the sum of this term over a static lattice with cubic symmetry is well known to be zero. Thus, only noncubic distortions of the crystal around the impurity can lead to nonzero orientational contributions. As will be discussed later, there are several such mechanisms, but they are most assuredly small at low pressures. This is supported by experimental evidence[1–6,9,14,15] which shows that the rotational states are very close to the free-rotor states of the isolated molecule. As for the intramolecular degrees of freedom, an inspection of Eq. (6) shows that the terms dependent on ξ are small compared to $V_{\text{intra}}(\xi)$ and thus represent a perturbation on the isolated molecule potential. Similarly, since the ξ-dependent terms in Eq. (6) are small compared to the term $k = 0$, the c.m. degrees of freedom are nearly decoupled from the orientational and intramolecular degrees of freedom. This suggests that the ground state of the system can be accurately described by the product function,

$$|\{\mathbf{R}_i\}, \theta, \xi\rangle = |\{\mathbf{R}_i\}\rangle\, |\theta\rangle\, |\xi\rangle \,, \tag{9}$$

where the $\{\mathbf{R}_i\}$ locate the instantaneous c.m. positions of the particles. Because of the relatively strong coupling of the X molecule to the Ar atoms, the center-of-mass motion can be accurately described by the Hartree expression, which is also known to be quite accurate for pure Ar crystals:[16]

$$|\{\mathbf{R}_i\}\rangle = \prod_{i=1}^{N} |\mathbf{R}_i\rangle \,, \tag{10}$$

where

$$|\mathbf{R}_i\rangle = \exp[-\alpha_i(\mathbf{R}_i - \mathbf{R}_i^0)^2/2] \tag{11}$$

and

$$|\theta\rangle = \sum_{J,M} C_{JM} Y_{JM}(\theta) \,. \tag{12}$$

Equation (12) is clearly appropriate since the rotational states are nearly free rotors for which the spherical harmonics Y_{JM} are eigenstates. The α_i and C_{JM} are variational coefficients to be determined. The equilibrium positions of the Ar atoms $\{R_i^0\}$, $i=2,3,\ldots,N$, must also be treated as variational parameters because of the distortion of the lattice around the impurity. Similar to $|\theta\rangle$, the state $|\xi\rangle$ can be described by an expansion using a harmonic-oscillator basis set.

The first step in the calculation is to determine the distortion of the host lattice around the X impurity. In this work the weak angular dependence of the X-Ar potential is neglected and, because of the weak coupling of the c.m. coordinates to ξ, the distortion is calculated using only the dominant term ($k,\lambda=0$) in Eq. (6). Hence, the calculation reduces to a simple Hartree impurity problem. Argon atoms in the first 16 shells around the molecule are allowed to relax to equilibrium,[17] and atoms beyond that range are assumed to have equilibrium positions identical to that of the pure lattice. Because of the uncorrelated nature of the product state given by Eq. (9), the distortion preserves the O_h symmetry experienced by the impurity, so the number of independent-symmetry coordinates that must be determined by optimization of the total energy reduces to 30. Thus,[17] the energy of the system is

$$E=(3\hbar^2/4)\left[(\alpha_1/m)+\sum_{i=2}^{N}(\alpha_i/M)\right]+\sum_{\substack{i,j=1\\ i<j}}^{N}[\alpha_{ij}/\pi(R_{ij}^0)^2]^{1/2}\int_{-\infty}^{\infty}(R_{ij}^0+Z)\exp(-\alpha_{ij}Z^2)V(R_{ij}^0+Z)dZ\ , \tag{13}$$

where

$$\alpha_{ij}=\alpha_i\alpha_j/(\alpha_i+\alpha_j)\ .$$

In the integral of Eq. (13), V_{1j}, $j=2,3,\ldots,N$, refers to Eq. (6) and, for $i,j=2,3,\ldots,N$, V_{ij} is represented by the Ar-Ar potential. To simplify the calculation α_1, associated with the molecule, and α_2 associated with the first-nearest-neighbor, argon atoms are treated as independent variational parameters. The α_i, $i=3,4,\ldots,N$, are assumed to be the same as for the pure rare-gas crystal and were determined by a subsidiary calculation. Thus, Eq. (13) was minimized with respect to the 30 symmetry coordinates $\{R_i^0\}$ and α_1 and α_2 at each of 30 different molar volumes. The one-dimensional integrals were evaluated using a Hermite quadrature routine, and lattice sums were taken out to a distance of five-nearest-neighbor lengths. The optimization of the energy in Eq. (13) with respect to the 30 symmetry coordinates and the two independent parameters α_1 and α_2 in the wave function is accomplished by a pattern recognition optimization at each volume of the multidimensional function $E(\alpha_1,\alpha_2,\{\mathbf{R}_i^0\})$. The details of this strategy are given elsewhere.[18] As will be shown in the next section, the lattice distortions are small and have only a minor effect on the predicted vibrational and rotational transition frequencies. The equilibrium position of the center of charge of the molecular impurity is assumed to be at a substitutional site in the argon host lattice which, except for HD, coincides with the position of the center of mass.

The analysis of the internal vibrational and rotational spectra of the trapped molecule is simplified by first taking the expectation value of the total relaxed Hamiltonian with respect to the product states $|\{\mathbf{R}_i\}\rangle|\theta\rangle$. Because of theoretical and experimental information presented earlier, the small anisotropies in the X-Ar potential are neglected, so the rotational states are given by those of a free rotor. Thus the only perturbation of the rotational states, caused by the crystal field of the host lattice, is due to the change in the rotational constant $B(\xi)$, given by Eq. (5). By expanding $B(\xi)$ in powers of ξ up to cubic terms, the resulting effective Hamiltonian, except for ignorable constants, becomes

$$H(\xi,J)=-\frac{\hbar^2}{2\mu}\nabla_\xi^2+\sum_{n=0}^{7}b_n\xi^n\ , \tag{14}$$

where

$$\begin{aligned}
b_0&=B_eJ(J+1)=(\hbar^2/2\mu r_e^2)J(J+1)\ ,\\
b_1&=\sum_{j=2}^{N}\langle V_{01}(R'_{1j})\rangle-2B_eJ(J+1)\ ,\\
b_2&=a_2+\sum_{j}\langle V_{02}(R'_{1j})\rangle+3B_eJ(J+1)\ ,\\
b_3&=a_3+\sum_{j}\langle V_{03}(R'_{1j})\rangle-4B_eJ(J+1)\ ,\\
b_i&=a_i,\ \ i=4,5,6,7\ ,
\end{aligned} \tag{15}$$

where $\langle V_{0k}(R'_{1j})\rangle=\langle\mathbf{R}_1,\mathbf{R}_j\,|\,V_{0k}\,|\,\mathbf{R}_1,\mathbf{R}_j\rangle$ is the Hartree integral over the c.m. motion of particles $(1,j)$.

We have calculated the eigenvalues E_{vJ} of Eq. (14) in several different ways that give very similar results. First, it is noted that Eq. (14) is in a form automatically suited for the Wentzel-Kramers-Brillouin (WKB) solution formulated by Dunham[19] which, by all accounts, is fairly accurate. Another method we have used is to solve the Schrödinger equation directly using the Numerov-Cooley method. That is,

$$\left[-\frac{\hbar^2}{2\mu}\left[\frac{\partial^2}{\partial r^2}+\frac{J(J+1)}{r^2}\right]+V(r)-E_{v,J}\right]\Phi_{vJ}(r)=0\ ,$$

where r is the intramolecular bond length and $V(r)$ is the sum of V_{intra} (Ref. 20) and

$$\sum_{j=2}^{N}\sum_{k=0}^{3}\langle V_{0k}(|\mathbf{R}'_1-\mathbf{R}_j^0|)\rangle\xi^k\ .$$

The third method is perturbation theory where the zeroth-order Hamiltonian is that of the free molecule, with the potential given by Eq. (7). This Hamiltonian is solved to obtain the exact eigenfunctions of the free molecule $\{|vJ\rangle\}$, and the frequencies of the transitions are given by the eigenvalues

$$\nu_{J'J''}^{v'v''}=E_{v'J'}^{0}-E_{v''J''}^{0} \; . \tag{16}$$

Then the perturbation given by the isotropic part of Eq. (6) is introduced. That is,

$$V'=\sum_{k=0}^{3}\sum_{j=2}^{N}\langle V_{0k}(R'_{1j})\rangle\xi^{k} \; , \tag{17}$$

where $\langle V_{0k}\rangle$ is the Hartree average over the center-of-mass motion of X and the argon atoms. The resulting frequency shifts between levels $v'J'$ and $v''J''$ are

$$\Delta\nu=\sum_{k}\sum_{j}\langle V_{0k}\rangle(\langle v'J'\,|\,\xi^{k}\,|\,v'J'\rangle-\langle v''J''\,|\,\xi^{k}\,|\,v''J''\rangle) \; . \tag{18}$$

Somewhat more accurate results can be achieved by recognizing that the leading term in the perturbation, Eq. (17), is the term $k=1$, linear in ξ. This term can be incorporated into the zeroth-order Hamiltonian, and by completing the square of this term and the quadratic term in V_{intra}, a better set of zeroth-order eigenfunctions can be obtained. All other terms are then treated as perturbations evaluated using lowest nonzero order perturbation theory.

The Dunham expansion[19] and the Schrödinger solutions give the vibrational and rotational states of the molecules in close agreement, as does the perturbation expansion at low pressures. At high pressure, the perturbation results are less accurate. For example, at $P=373$ kbar the calculated frequency shifts of the $S_0(0)$ and $Q_1(0)$ transitions, based upon the perturbation method, are 10.3% and 14% higher than those determined using the more accurate Dunham-expansion and Schrödinger-solution methods. In this work only the results of the Dunham expansion[19] will be reported.

HD impurities present a special calculational problem in that the charge center and the c.m. are displaced from one another by a distance $r/6$. However, the single-particle orbital $|\,\mathbf{R}_1\rangle$ is properly centered about the c.m. equilibrium position $\mathbf{R}_1^0$, but the interaction between the molecule and the jth host lattice atom depends on the distance between the charge center and the c.m. of the jth atom. That is, $\mathbf{R}'_{1j}=\mathbf{R}_{1j}+(r/6)\hat{\mathbf{u}}$, where $\hat{\mathbf{u}}$ is a unit vector giving the direction between the molecular c.m. and the center of charge. In this work it was assumed that because the rotational states are nearly isotropic, the charge center uniformly samples a spherical surface of radius $(r/6)$ about the center of mass, and so $\hat{\mathbf{u}}$ is averaged over this surface by integrating over the solid angle $d\Omega_{\hat{\mathbf{u}}}$. This can be accomplished by either expressing $|\,\mathbf{R}_1\rangle$ in terms of $\hat{\mathbf{u}}$ and $\mathbf{R}'_1$ or transforming Eq. (6) to a function of the center-of-mass position $V(\mathbf{R}_{1j},\hat{\mathbf{u}},\theta_{1j},\xi)$, as was done in this calculation.

Within the Hartree approximation it is also possible to calculate the local-mode frequency of the molecular impurity in the cage produced by the surrounding argon atoms. It is given by

$$\nu_{\text{c.m.}}(\text{cm}^{-1})=\alpha_1(\hbar/mc) \; , \tag{19}$$

where c is the velocity of light.

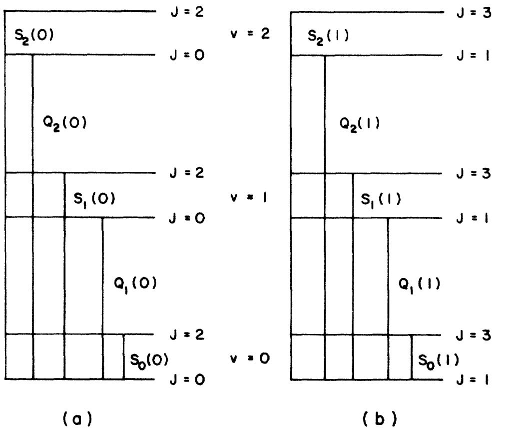

FIG. 1. Rotational and vibrational transitions for (a) para-H_2 and ortho-D_2 and (b) ortho-H_2 and para-D_2. J and v are the rotational and vibrational quantum numbers, respectively.

III. RESULTS

Figure 1 shows the transitions investigated in this work, where (v,J) correspond to the vibrational and rotational quantum numbers that characterize the states of the molecule. Thus Fig. 1(a) identifies those transitions allowable for para-H_2 and ortho-D_2, and Fig. 1(b) is for ortho-H_2 and para-D_2. Since HD is not homonuclear all transitions [Figs. 1(a) and 1(b)] are allowed.

The first stage of the calculation involved relaxing to equilibrium the first 16 shells of argon atoms around the impurity and evaluating the wave-function parameters α_1, α_2, and α_3 which minimize the crystal energy, Eq. (13). At zero pressure, $V\simeq 22.5$ cm^3/mole, the ratios of the H_2-Ar bond lengths of the first 16 neighboring Ar shells, to those for a pure argon lattice are 0.9942, 1.0010, 0.9993, 1.0001, 0.9997, 0.9998, 1.0000, 0.9998, 1.0000, 1.0000, 0.9999, 1.0000, 0.9999, 1.0000, 1.0000, and 1.0000, and the parameters α_1, α_2, and α_3 equal to 7.62, 57.02, and 58.25 Å^{-2}, respectively. At $P=373$ kbar the bond-

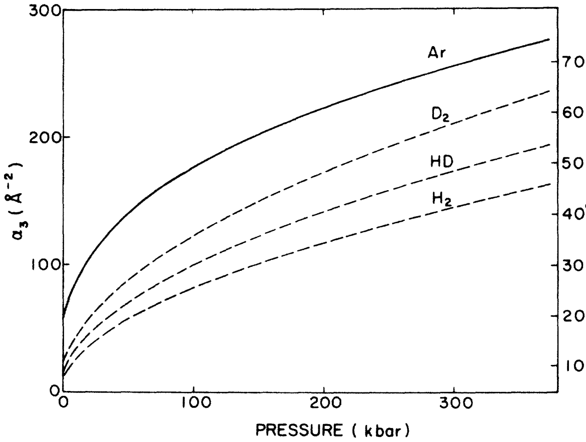

FIG. 2. The solid line gives the variational parameter α_3 in the wave function for pure solid Ar versus pressure. The dashed lines, from top to bottom are the variational parameters for the D_2, HD, and H_2 impurity wave functions, respectively.

length ratios for the first five shells are 0.981, 1.001, 0.997, 0.997, and 1.000. Thus, the lattice distortion is very small and remains so for all calculated pressures. This is also true for D_2 and HD in argon. However, the parameters $(\alpha_1,\alpha_2,\alpha_3)$ strongly increase with pressure and depend on the impurity species, as shown in Fig. 2. This will be shown to be an important factor in the analysis of the transition frequencies. The dashed lines in Fig. 2 show the α_1 (right-hand scale) for H_2, HD, and D_2, versus pressure, and the solid line (left-hand scale) shows α_3 for pure argon. α_2, not shown, is from 1.1 to 1.25 Å^{-2} lower than α_3 over the entire pressure range. From the values of α_1 the local-mode frequencies can be calculated at all pressures using Eq. (19).

Table I shows the vibrational and rotational transition frequencies calculated in this work at zero temperature versus molar volume and pressure. The pressures are determined by differentiating a polynomial fit of the

TABLE I. Frequency shifts (cm^{-1}) with respect to gas-phase values versus molar volume (cm^3/mole), for vibrational, rotational, and rotational-vibrational transitions of H_2, D_2, and HD impurities in solid argon. Pressures are in kbar.

P	Volume	$S_0(0)$	$S_0(1)$	$Q_1(0)$	$Q_1(1)$	$S_1(0)$	$S_1(1)$	$Q_2(0)$	$Q_2(1)$	$S_2(0)$	$S_2(1)$
					H_2-Ar						
0.11	22.5	−1.77	−2.94	−21.04	−21.01	−22.72	−23.80	−39	−39	−41	−42
0.86	22.0	−1.73	−2.88	−19.94	−19.90	−21.57	−22.60	−37	−36	−38	−39
2.86	21.0	−1.62	−2.69	−16.80	−16.75	−18.27	−19.18	−30	−29	−31	−32
5.72	20.0	−1.42	−2.35	−12.02	−11.95	−13.23	−13.95	−19	−19	−20	−21
9.80	19.0	−1.10	−1.82	−4.96	−4.86	−5.77	−6.20	−4	−4	−4	−5
15.60	18.0	−0.61	−1.01	5.29	5.42	5.06	5.06	18	18	18	19
23.85	17.0	0.11	0.20	20.00	20.17	20.63	21.25	49	49	50	52
35.66	16.0	1.17	1.97	41.02	41.26	42.90	44.41	93	94	96	98
52.64	15.0	2.73	4.57	71.04	71.36	74.72	77.52	156	157	161	165
77.27	14.0	5.00	8.35	114.01	114.44	120.29	124.92	246	247	254	260
113.37	13.0	8.32	13.88	175.74	176.31	185.78	193.06	375	376	387	396
167.03	12.0	13.20	22.01	264.88	265.66	280.40	291.52	561	562	579	593
248.18	11.0	20.41	34.02	394.41	395.45	417.94	434.65	829	832	857	877
373.37	10.0	31.17	51.92	583.76	585.16	619.11	644.02	1221	1224	1261	1291
					D_2-Ar						
	22.5	−0.97	−1.61	−17.35	−17.35	−18.30	−18.91	−34	−34	−34	−35
	22.0	−0.96	−1.59	−16.75	−16.74	−17.67	−18.27	−32	−32	−33	−34
	21.0	−0.91	−1.52	−14.90	−14.89	−15.77	−16.33	−28	−28	−29	−30
	20.0	−0.83	−1.37	−11.97	−11.95	−12.73	−13.21	−22	−22	−23	−23
	19.0	−0.69	−1.14	−7.50	−7.47	−8.09	−8.45	−12	−12	−13	−13
	18.0	−0.47	−0.77	−0.88	−0.84	−1.22	−1.40	1	2	1	1
	17.0	−0.13	−0.21	8.77	8.82	8.81	8.90	22	22	22	22
	16.0	0.37	0.63	22.71	22.79	23.31	23.80	51	51	51	52
	15.0	1.11	1.86	42.82	42.92	44.24	45.30	92	93	94	96
	14.0	2.20	3.67	71.81	71.95	74.43	76.32	152	153	155	158
	13.0	3.80	6.34	113.73	113.92	118.10	121.21	239	239	244	248
	12.0	6.17	10.29	174.60	174.86	181.54	186.43	364	365	372	378
	11.0	9.69	16.15	263.49	263.84	274.22	281.73	547	547	559	567
	10.0	14.96	24.93	394.04	394.51	410.41	421.78	814	815	832	845
					HD-Ar						
	22.5	−1.27	−2.11	−16.09	−16.06	−17.26	−18.01	−29	−29	−30	−31
	22.0	−1.23	−2.05	−14.82	−14.79	−15.95	−16.65	−26	−26	−27	−28
	21.0	−1.12	−1.86	−11.34	−11.29	−12.31	−12.89	−19	−18	−19	−20
	20.0	−0.94	−1.56	−6.18	−6.12	−6.92	−7.33	−7	−7	−8	−8
	19.0	−0.66	−1.09	1.26	1.35	0.88	0.72	9	9	9	9
	18.0	−0.24	−0.38	11.89	12.01	12.02	12.24	32	32	32	33
	17.0	0.38	0.65	26.96	27.12	27.83	28.58	64	64	65	66
	16.0	1.28	2.16	48.28	48.49	50.21	51.72	109	109	112	114
	15.0	2.59	4.34	78.45	78.73	81.90	84.50	173	173	177	181
	14.0	4.49	7.50	121.24	121.62	126.87	131.01	263	263	269	275
	13.0	7.24	12.09	182.17	182.67	190.92	197.27	390	391	401	409
	12.0	11.26	18.78	269.29	269.96	282.55	292.07	572	573	588	599
	11.0	17.16	28.61	394.44	395.32	414.25	428.35	832	834	855	872
	10.0	25.89	43.15	574.96	576.12	604.33	625.06	1206	1208	1239	1264

TABLE II. Measured Raman frequency shifts from gas-phase values (cm^{-1}) at zero pressure for H_2, D_2, and HD impurities in solid argon at temperature 12–15 K. Data taken from Refs. 2 and 1, the latter in parentheses. Impurity local-mode frequencies $\nu_{\mathrm{c.m.}}$ are calculated at zero temperature.

System	$S_0(0)$	$S_0(1)$	$Q_1(0)$	$Q_1(1)$	$S_1(0)$	$S_1(1)$	$\nu_{\mathrm{c.m.}}$	$\nu_{\mathrm{c.m.}}$ (theory)
H_2(Ar)	3.6	3.9	−23.1		−17.7	−19.8	112[a]	127
	(−2.3)	(−2.86)	(−17.93)	(−18.3)				
D_2(Ar)	−6.1	−0.52	−16.6	−14.45	−16.3	−13.4	79[b]	84.4
	(−0.16)	(0.68)	(−20.4)	(−20.35)				
HD(Ar)	7.9		−13.1		−3.5			92.6

[a] Measured at 82 K.

[b] Measured at 80 K.

energy-volume results. The listed frequencies represent the shift from gas-phase values given by Stoicheff.[14] Most notable in these results is that the pure vibrational and vibrational-rotational transitions are strongly red-shifted in the solid at pressure $P=0$, compared to the gas phase. These results can be compared to the observed Raman scattering data of Prochaska and Andrews[2] and Jodl and Bier[1] (values within parenthesis), shown in Table II. The calculated pure rotational transition frequencies show a small red shift at $P=0$ in the solid compared to their gas-phase values, and comparisons with experimental data[1,2] displayed in Table II can also be made. The calculated and observed[2] local-mode frequencies, $\nu_{\mathrm{c.m.}}$, are also shown in Table II.

At pressures $P\neq 0$, all the calculated transitions shown in Table I are strongly blue-shifted with respect to their $P=0$ solid values. The solid lines in Fig. 3 show our calculated P-V relation at 0 K. The circles represent measurements[21] taken at 4 K, and the squares[22] and triangles[23] are room-temperature measurements. The solid and dashed lines in Fig. 4 show the pressure dependence of the $Q_1(0)$ transition frequency for H_2 and D_2, respectively. These curves are almost identical to those for the $Q_1(1)$ transition. The frequencies for HD are quite close to those for H_2 and are therefore not shown.

IV. CONCLUSIONS AND DISCUSSION

An inspection of Table II shows that there exists considerable divergence in the transition frequencies observed at $P=0$ from different Raman scattering experiments[1,2] and, in many cases, these differences are outside the reported uncertainties. In the work of Prochaska and Andrews[2] two lines at 4138 and 4144 cm^{-1} were observed for H_2(Ar), and they argued that the 4138-cm^{-1} line corresponded to $Q_1(0)$ and the 4144-cm^{-1} lines are due to molecular aggregates. Jodl and Bier[1] have argued that these identifications are incorrect, and that the 4144-cm^{-1} line is the $Q_1(0)$ mode and the 4138-cm^{-1} line is the $Q_1(1)$ mode. If so, then Prochaska and Andrew's data would give 17.13 and 17.20 cm^{-1} for the $Q_1(0)$ and $Q_1(1)$ frequency shifts, respectively, which puts the two experiments into good agreement for these modes. A comparison of our calculated results for (H_2,D_2,HD)Ar

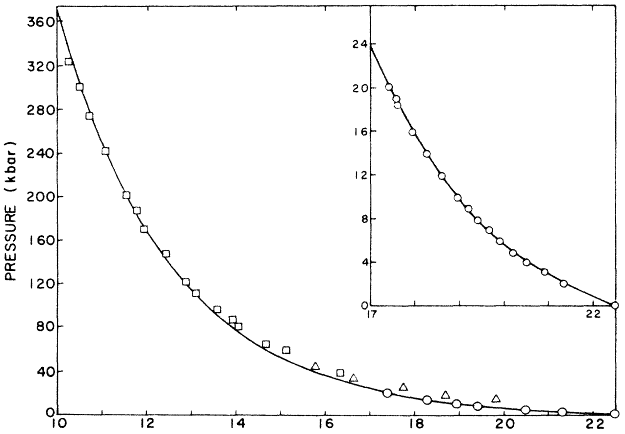

FIG. 3. The solid lines are the calculated pressure-volume curves along the zero-temperature isotherm for solid argon. The circles are experimental measurements (Ref. 21) at $T=4$ K, and the squares (Ref. 22) and triangles (Ref. 23) are room-temperature measurements. The inset is an expansion of the low-pressure region.

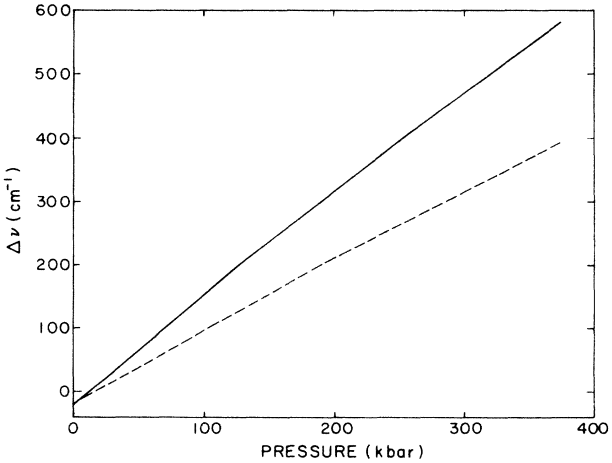

FIG. 4. The frequency change of the $Q_1(0)$ transition versus pressure for H_2 (solid line) and D_2 (dashed line). The HD results are very close to the solid line and results for $Q_1(1)$ are nearly identical to those for $Q_1(0)$.

and experiment[1,2] for these pure vibrational transitions agrees with experiment and are well within the uncertainty in the measurements. Moreover, the calculations show that the shifts in $Q_1(0)$ and $Q_1(1)$ are nearly the same, which most closely agrees with the measurements of Jodl and Bier,[1] although it is puzzling that they measure larger shifts for D_2 than for H_2. This is contrary to our expectations and to our results.

The calculated frequency shifts of the pure rotational transitions, $S_0(0)$ and $S_0(1)$ in the solid at zero pressure, also show red shifts for all the isotopic impurities. These calculated shifts are small and they agree well with the experimental data of Jodl and Bier,[1] but not so well with the measurements of Prochaska and Andrews,[2] who get blue shifts for H_2(Ar) and HD(Ar). In the latter case the measured blue shift is quite large. It is not possible to say at this point which of the experiments is most accurate, but it does have an important bearing on our understanding of this system. Recall that the orientational term in the potential that couples the molecule to the host lattice was neglected in this calculation, so the only crystal-field effect that perturbs the rotational states is the change in the rotational constant via a change in the intramolecular bond length, which increases with respect to r_e in the solid at $P=0$. Thus, the only possible outcome from a calculation is a red shift, and any reliable measured data that gives another result must be a consequence of the potential anisotropy.

The calculated vibrational-rotational transitions $S_1(0)$ and $S_1(1)$ are also strongly red-shifted at $P=0$, and while the agreement with experiment[2] is not as good as for the pure vibrational transitions, it is, with the exception of $S_1(0)$ for HD, reasonable. The drastic discrepancy for this mode is not understood. The calculated shifts for the higher transitions $Q_2(0)$, $Q_2(1)$, $S_2(0)$, and $S_2(1)$ have not been experimentally measured.

The calculated local-mode frequencies at $P=0$ in the solid are in good agreement with experiment, as shown on Table II, although care must be taken because the measurements[2] are at 80 K and the calculations are at zero temperature. In fact, there is clear evidence[8] that these frequencies $\nu_{\text{c.m.}}$ increase considerably with decreasing temperature, and by extrapolating the experimental values to zero temperature it is evident that our calculated results should agree even more closely with experiment.

Our calculations for each of the isotopic impurities were extended to pressures $0 \leq P \leq 373$ kbar. An examination of Table I shows that all the modes exhibit very strong monotonic blue shifts with increasing pressure. In fact, $d\nu/dP$ is approximately 3–4 times larger than for O_2, N_2, CO, and CO_2 in their own lattices.[24] These large shifts are no doubt due to the relatively strong repulsion at small separations in the X-Ar potential. One interesting feature of these results has to do with the fact that the $Q_1(0)$ mode of H_2 in its own solid lattice increases in frequency up to approximately 330 kbar and then softens and begins to decrease,[25] at least up to the limits of the measurements at about 600 kbar. One may speculate that this is due to the onset of the often-predicted molecular-to-atomic phase transitions in solid hydrogen where it is reasonable to assume that the charge distribution of the molecule becomes altered by the crystal field of the surrounding molecules, thus weakening the intramolecular bond. Because the interrelationship between the intramolecular and intermolecular forces in the H_2-H_2 interaction is not well known, especially in the condensed state, a direct test of this hypothesis is not presently possible. On the contrary, this interrelation is well known for H_2-Ar because of the work of LeRoy and Carley,[9] at least for isolated pairs. Thus, a question can be posed. Is the turnover in $Q_1(0)$ in pure solid H_2 only a consequence of the large external pressure of the crystal field on an H_2 molecule, in which case the turnover should be seen for H_2 in solid Ar also, or is it a special feature of H_2-H_2 interactions themselves? Our results show no evidence of a turnover in $Q_1(0)$ for H_2 in Ar up to 373 kbar.

There is a feature in our calculations that has a bearing on the above discussions. It is almost certainly true that the orientational interaction in the X-Ar potential contributes at most a negligibly small amount to perturbing the vibrational and rotational states of the hydrogen molecule in solid Ar at $P=0$. The observed magnitude of the rotational frequency shifts, and the lack of evidence for a splitting of the rotational levels is consistent with this argument. However, the coupling constants $V_{2k}(R'_{1j})$ in the orientational part of Eq. (6) clearly increase strongly with increasing pressure so that even small noncubic distortions of the crystal field may become important at high pressures. If so, the perturbation of the rotational states could, under the most drastic circumstances, lead to an orientational order-disorder transition at high pressures, as occurs in pure bulk hydrogen.[25,26] An inspection of the X-Ar potential[9] leads to the conclusion that the vibrational states would not be significantly altered by such an occurrence, but the rotational eigenstates most surely would. Clearly, the only way the orientational interaction can contribute to system properties is via a correlation between the c.m. and orientational degrees of freedom, which is missing in our uncorrelated product wave function. In principle, it is possible to solve this difficult problem, but it is presently unclear as to what approach would be most tractable. Experimental information about the rotational transitions at high pressure would greatly elucidate this problem and test the validity of the above-mentioned conjecture.

The Ar-Ar pair potential V_{Ar} used in this work is taken from the electron-gas work of LeSar[12] and is fitted so that the well and long-range region closely agrees with the excellent work of Aziz and Chen, and Barker and Bobetic.[13] In this way the known departure in the condensed phase of the short-range repulsive region, given by accurate isolated pair potentials, is properly described. As shown by Fig. 3, the calculated pressure-volume relation is in excellent agreement with low-temperature measurements[21] and with room-temperature data[22,23] when thermal corrections are accounted for, as provided by Zou *et al.*[22] and Finger *et al.*[23] Note that the room-temperature data coincides with our zero-temperature isotherm mentioned above, approximately 100 kbar, where thermal corrections are relatively small. Thus, it is expected that the calculated pressures are quite accurate. Regardless, the volume dependence of the frequency shifts depends almost entirely on the Hartree average of $V_{0k}(R'_{1j})$ and only very weakly on the details of the short-ranged part of the V_{Ar}, as has been verified by calculation.

Finally, we have examined various special cases of our theory in order to better understand the important features of the problem. In one case, an Einstein approximation was used in which the Ar atoms are fixed classically at their relaxed equilibrium lattice sites. In that case the Hartree averages in Eqs. (15) are of the form $\langle \mathbf{R}_1 | V_{0k}(| \mathbf{R}_1' - \mathbf{R}_j^0 |) | \mathbf{R}_1 \rangle$ which reduces to simple one-dimensional integrals. The results for the various transition frequencies and the local-mode frequencies are quite close to the full Hartree approximation characterized by Eqs. (9)—(12). An examination of the α_1 shows why this is so. That is, $\alpha_1 \ll \alpha_i$, $i=2,3,\ldots$, so that the rms c.m. fluctuations of the argon atoms are very small compared to hydrogen and can, to a first approximation, be neglected. A more drastic approximation, which treats the c.m. motion of the molecular impurity as well as the argon atoms classically, was also carried out. In this case, the $\sum_j \langle V_{0k} \rangle$ in Eqs. (15) become simple classical lattice sums. Here, the error is dramatic. For example, the shift in the $Q_1(0)$ mode for H_2 at $P=0$ for this case is -33 cm^{-1}, compared to -21.04 cm^{-1} based upon the full Hartree average. Thus, averaging the contributions $\sum_j \langle V_{0k}(\mathbf{R}')_{1j} \rangle$ over at least the c.m. motion of the hydrogen impurity is vital in obtaining accurate results.

In summary, we have predicted the frequency shifts of all the low-lying vibrational-rotational transitions of H_2, D_2, and HD over a wide range of pressures, and the agreement with experiment[1,2] has been generally quite good, although a few unexplained exceptions exist. In this work we have taken advantage of the most recent descriptions of the X-Ar potential,[9] and the intramolecular potentials have been expanded out to seventh order in the bond-length displacement from equilibrium, which was determined to be necessary to achieve the desired accuracy. In addition, the relaxation of the host lattice around the impurity was calculated to high accuracy. It is evident that additional experimental information that gives the frequencies of a larger number of rotational and vibrational states than is now available would be highly desirable in the solid at $P=0$ and at high pressures.

ACKNOWLEDGMENTS

The authors would like to thank Dr. Robert LeRoy for his assistance on this problem and to the Cray GC$_2$ VR group for providing computational facilities. One of us, R.D.E., would also like to thank Los Alamos National Laboratory for their hospitality, where this work was completed. This work was partially supported by the U.S. Department of Energy under Contract No. DE-AC02-84ER45050.

---

[1] H. Jodl and K. Bier, *Vibrational Spectra and Structure,* edited by J. R. Durig (Elsevier, New York, 1984), Vol. 13, p. 285.

[2] G. Prochaska and L. Andrews, J. Chem. Phys. **67**, 1139 (1977).

[3] R. Kriegler and H. Welsh, Can. J. Phys. **46**, 1181 (1968).

[4] J. DeRemigis and H. Welsh, Can. J. Phys. **48**, 1622 (1970).

[5] J. Warren, G. Smith, and W. Guillory, J. Chem. Phys. **72**, 4901 (1980).

[6] G. Smith, J. Warren, and W. Guillory, J. Chem. Phys. **65**, 1591 (1976).

[7] M. Jean-Louis and H. Vu, *International Phonon Conference Proceedings, Rennes, France,* edited by M. Nusimovica (Flammarion, Paris, 1971), p. 268.

[8] J. Vitko, Jr. and C. F. Coll, J. Chem. Phys. **69**, 2590 (1978).

[9] R. LeRoy and J. Carley, *Advances in Chemical Physics,* edited by K. P. Lawley (Wiley, New York, 1980), p. 353.

[10] J. van Kranendonk, Rev. Mod. Phys. **40**, 531 (1976).

[11] G. Herzberg, *Spectra of Diatomic Molecules* (Van Nostrand/Reinhold, New York, 1950).

[12] R. LeSar, J. Phys. Chem. **88**, 4272 (1984).

[13] R. Aziz and H. Chen, J. Chem. Phys. **67**, 5719 (1977); J. A. Barker and M. V. Bobetic, *ibid.* **79**, 6306 (1983).

[14] B. P. Stoicheff, Can. J. Phys. **35**, 730 (1957).

[15] A. McKellar and H. Welsh, Can. J. Phys. **50**, 1458 (1972).

[16] L. H. Nosanow and G. L. Shaw, Phys. Rev. **128**, 546 (1962).

[17] M. Derbyshire and R. D. Etters, J. Chem. Phys. **79**, 831 (1983).

[18] R. P. Pan and R. D. Etters, J. Chem. Phys. **72**, 1741 (1980).

[19] J. L. Dunham, Phys. Rev. **41**, 721 (1932).

[20] D. M. Bishop and S. K. Shih, J. Chem. Phys. **64**, 162 (1976).

[21] M. S. Anderson and C. A. Swenson, J. Phys. Chem. Solids **36**, 145 (1975).

[22] G. Zou, H. K. Mao, and P. M. Bell, *Carnegie Institution of Washington Yearbook* (Carnegie Institute, Washington, D.C., 1982), p. 392.

[23] L. W. Finger, R. M. Hazen, G. Zou, H. K. Mao,and P. M. Bell, Appl. Phys. Lett. **39**, 892 (1981).

[24] R. D. Etters and A. A. Helmy, Phys. Rev. B **27**, 6439 (1983), and references therein.

[25] S. Sharma, H. Mao, and P. Bell, Phys. Rev. Lett. **44**, 886 (1980); I. F. Silvera and R. J. Wijngaarden, *ibid.* **47**, 39 (1981).

[26] J. Raich and R. D. Etters, J. Low Temp. Phys. **6**, 229 (1972); W. England, J. Raich, and R. D. Etters, *ibid.* **22**, 213 (1976); J. Silvera and R. Wijngaarden, Phys. Rev. Lett. **47**, 39 (1981).